Formation and Characterization of the Oxygen-Rich Scandium Oxide/Dioxygen Complexes ScO_n ($n = 4, 6, 8$) in Solid Argon

Yu Gong, Chuanfan Ding, and Mingfei Zhou*

Department of Chemistry, Shanghai Key Laboratory of Molecular Catalysts and Innovative Materials, Advanced Materials Laboratory, Fudan University, Shanghai 200433, P. R. China

Received: July 12, 2007; In Final Form: August 30, 2007

The reactions of scandium atoms and O_2 have been reinvestigated using matrix isolation infrared spectroscopy and density functional theory calculations. A series of new oxygen-rich scandium oxide/dioxygen complexes were prepared and characterized. The ground state scandium atoms react with dioxygen to form $OSc(\eta^2\text{-}O_3)$, a side-on bonded scandium monoxide-ozonide complex. The $OSc(\eta^2\text{-}O_3)$ complex rearranges to a more stable $Sc(\eta^2\text{-}O_2)_2$ isomer under visible light irradiation, which is characterized to be a side-on bonded superoxo scandium peroxide complex. The homoleptic trisuperoxo scandium complex, $Sc(\eta^2\text{-}O_2)_3$, and the superoxo scandium bisozonide complex, $(\eta^2\text{-}O_2)Sc(\eta^2\text{-}O_3)_2$, are also formed upon sample annealing. The $Sc(\eta^2\text{-}O_2)_3$ complex is determined to have a D_{3h} symmetry with three equivalent side-on bonded superoxo ligands around the scandium atom. The $(\eta^2\text{-}O_2)Sc(\eta^2\text{-}O_3)_2$ complex has a C_2 symmetry with two equivalent side-on bonded O_3 ligands and one side-on bonded superoxo ligand.

Introduction

The reactions of transition metals and O_2 are of great interest in catalytic oxidation and biological systems. Numerous studies have been devoted to the investigation of the electronic and geometric structures and reactivities of transition metal oxides and dioxygen complexes.[1] Scandium is the first transition metal element in the periodic table with only one d electron, which can serve as a starting point for understanding the metal−oxygen bonding in the other more complicated transition metal oxides and dioxygen complexes. The scandium monoxide molecule was investigated both theoretically[2−8] and experimentally.[9−14] The ground state as well as spectroscopic constants of ScO have been obtained. The equilibrium geometry of the ground state of ScO_2 has been the subject of several theoretical calculations.[15,16] Although a symmetry-broken C_s equilibrium structure was predicted to lie lower in energy than the bent C_{2v} structure, high-level theory predicted that it is unlikely the symmetry-broken C_s structure is experimentally detectable.[14,17,18] Experimentally, a 722 cm^{-1} absorption from the reaction of laser-ablated scandium atoms with dioxygen was attributed initially to the antisymmetric stretching mode of the C_{2v} ScO_2 molecule in solid argon,[13] but it has been reassigned to the ScO_2^- anion.[14] Besides the ScO and ScO_2 molecules, higher scandium oxides and dioxygen complexes have also been reported. An anion photoelectron spectroscopic study was performed on the ScO_n^- ($n = 1-4$) species.[19] The PES spectra of the higher oxide species (ScO_3 and ScO_4) were found to be quite broad and featureless, which were assigned to different O_2 complexes of the metal atom and monoxide. In the matrix isolation infrared spectroscopic study on the reaction of laser-ablated scandium atoms with O_2, higher oxide species were also reported.[13] Two isomers of ScO_3, a dioxygen complex of monoxide and an ozonide complex, were observed. The observed ScO_4 species was attributed to an $Sc(O_2)_2$ complex with two equivalent molecular oxygens. However there is no report on the oxygen-rich ScO_n species with $n > 4$.

Recent investigations in this laboratory on the reactions of group IVB metal atoms with dioxygen have shown that the metal atoms reacted with dioxygen directly to give initially the inserted metal dioxide molecules, which further reacted with dioxygen to form the unprecendented oxygen-rich MO_6 and MO_8 species for the experiments with excess oxygen.[20] In this paper, we provide a joint matrix isolation infrared spectroscopic and theoretical study on the reaction of scandium atoms and O_2. A series of new oxygen-rich scandium oxide/dioxygen complexes were prepared and identified.

Experimental and Computational Methods

The experimental setup for pulsed laser-evaporation and matrix isolation infrared spectroscopic investigation has been described in detail previously.[21] Briefly, the 1064 nm fundamental of a Nd:YAG laser (Continuum, Minilite II, 10 Hz repetition rate, and 6 ns pulse width) was focused onto a rotating scandium target through a hole in a CsI window cooled normally to 6 K by means of a closed-cycle helium refrigerator (ARS, 202N). The laser-evaporated scandium atoms were co-deposited with oxygen/argon mixtures onto the CsI window. In general, matrix samples were deposited for 1 to 1.5 h at a rate of approximately 4 mmol/h. The O_2/Ar mixtures were prepared in a stainless steel vacuum line using standard manometric technique. Isotopic $^{18}O_2$ (ISOTEC, 99%) was used without further purification. The infrared absorption spectra of the resulting samples were recorded on a Bruker IFS 66V spectrometer at 0.5 cm^{-1} resolution between 4000 and 450 cm^{-1} using a liquid nitrogen cooled HgCdTe (MCT) detector. Samples were annealed at different temperatures and subjected to broadband irradiation using a high-pressure mercury arc lamp with glass filters.

Quantum chemical calculations were performed using the Gaussian 03 program.[22] The three-parameter hybrid functional

* Corresponding author. E-mail: mfzhou@fudan.edu.cn.

10.1021/jp075470v CCC: $37.00
Published on Web 10/16/2007

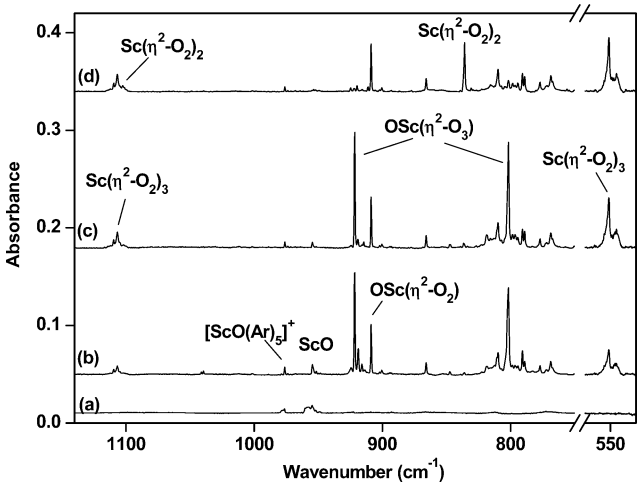

Figure 1. Infrared spectra in the 1140−750 and 580−520 cm^{-1} regions from co-deposition of laser-evaporated scandium atoms with 0.1% O_2 in argon: (a) 1 h of sample deposition at 6 K, (b) after 30 K annealing, (c) after 40 K annealing, and (d) after 15 min of $400 < \lambda < 580$ nm irradiation.

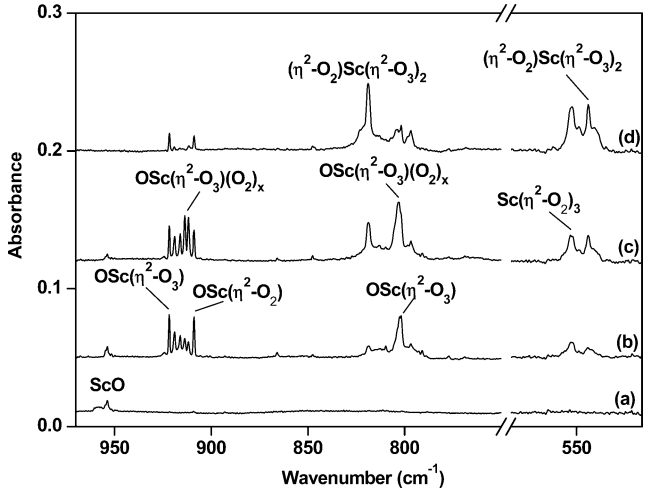

Figure 2. Infrared spectra in the 970−780 and 580−520 cm^{-1} regions from co-deposition of laser-evaporated scandium atoms with 0.25% O_2 in argon: (a) 1 h of sample deposition at 6 K, (b) after 25 K annealing, (c) after 30 K annealing, and (d) after 40 K annealing.

according to Becke with additional correlation corrections due to Lee, Yang, and Parr (B3LYP) was utilized.[23,24] The 6-311+G-(d) basis set was used for the O atom, and the all-electron basis set of Wachters−Hay as modified by Gaussian was used for the Sc atom.[25] The geometries were fully optimized; the harmonic vibrational frequencies were calculated, and zero-point vibrational energies (ZPVE) were derived. Transition state optimization was done with the synchronous transit-guided quasi-Newton (STQN) method at the B3LYP/6-311+G(d) level.

Results and Discussion

Infrared Spectra. A series of experiments were performed with different O_2 concentrations and laser energies. The infrared spectra in selected regions using 0.1% O_2 in argon with approximately 5 mJ/pulse laser energy are shown in Figure 1. After 1 h of sample deposition at 6 K, weak absorptions at 722.5, 954.8, and 976.3 cm^{-1} were observed (Figure 1, trace a). The 954.8 cm^{-1} band was previously assigned to the ScO absorption.[13] The 722.5 cm^{-1} band was attributed initially to the ScO_2 neutral,[13] but it has been reassigned to the ScO_2^- anion.[14] The 976.3 cm^{-1} band was previously assigned to the ScO^+ cation absorption,[14] but recent investigation indicated that the ScO^+ cation trapped in solid argon should be regarded as an isolated $[ScO(Ar)_5]^+$ complex.[26] When the as-deposited sample was annealed to 30 K (Figure 1, trace b), absorption at 908.8 cm^{-1}, which was previously identified as $OSc(\eta^2\text{-}O_2)$, was produced.[13] In addition, new absorptions at 1106.7, 921.7, 801.8, and 551.7 cm^{-1} were produced. These new product absorptions can be divided into two groups based on their behavior upon sample annealing and irradiation. The 1106.7 and 551.7 cm^{-1} absorptions markedly increased upon sample annealing to 40 K (Figure 1, trace c) and remained almost unchanged on subsequent visible light irradiation (Figure 1, trace d). The 921.7 and 801.8 cm^{-1} absorptions increased together on sample annealing and disappeared upon visible light irradiation, during which a group of new absorptions at 1102.4, 836.0, 631.7, and 612.7 cm^{-1} were produced.

Figure 2 shows the spectra with 0.25% O_2 in argon using the same laser energy as in the experiment shown in Figure 1. The ScO, ScO_2^-, and $[ScO(Ar)_5]^+$ absorptions were also observed after sample deposition, and the 1106.7, 921.7, 801.8, and 551.7 cm^{-1} absorptions were produced on sample annealing.

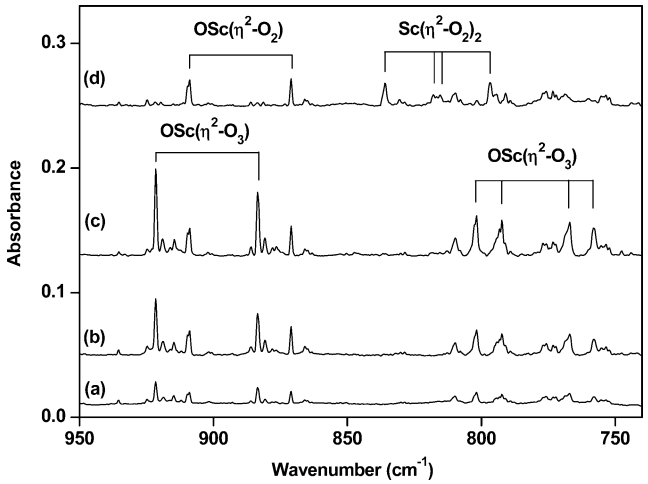

Figure 3. Infrared spectra in the 950−740 cm^{-1} region from co-deposition of laser-evaporated scandium atoms with 0.05% $^{16}O_2$ + 0.05% $^{18}O_2$ in argon: (a) 1.5 h of sample deposition at 6 K, (b) after 25 K annealing, (c) after 35 K annealing, and (d) after 15 min of $400 < \lambda < 580$ nm irradiation.

Four new absorptions at 919.0, 916.1, 913.8, and 911.9 cm^{-1} appeared on sample annealing. The intensities of the low-frequency absorptions increased at the expense of the high-frequency absorptions and the 921.7 cm^{-1} absorption when the matrix sample was annealed to higher temperatures. The 801.8 cm^{-1} band is broadened and the peak position shifted to 803.5 cm^{-1} when the matrix sample was annealed to 30 K. The 919.0, 916.1, 913.8, 911.9, and 803.5 cm^{-1} absorptions disappeared when the matrix sample was annealed to 40 K (Figure 2, trace d), while a set of new absorptions at 818.7, 681.2, 678.7, and 544.6 cm^{-1} markedly increased.

The experiments were repeated by using the isotopic labeled $^{18}O_2$ sample and the $^{16}O_2 + {}^{18}O_2$ and $^{16}O_2 + {}^{16}O^{18}O + {}^{18}O_2$ mixtures. The spectra in selected regions with different isotopic samples are shown in Figures 3−5, respectively. The band positions of the new product absorptions are summarized in Table 1.

$OSc(\eta^2\text{-}O_3)$. The 921.7 and 801.8 cm^{-1} absorptions dominated the spectrum after annealing with relatively low O_2 concentrations. These two absorptions were previously assigned to the $(O_2)_xScO$ and ScO_3 species.[13] However, these two absorptions exhibited constant relative intensities throughout all

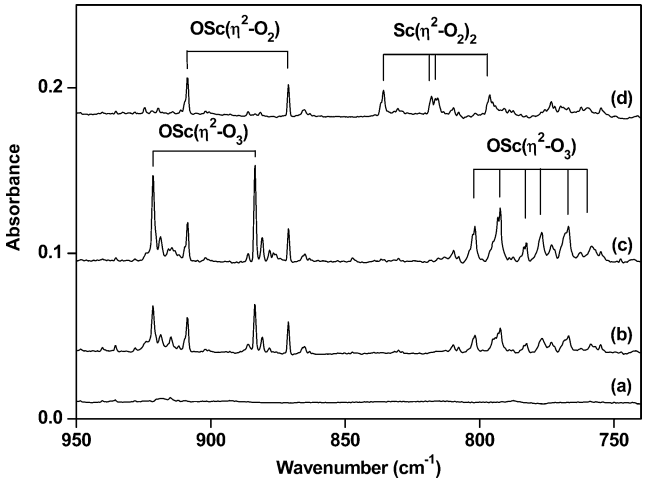

Figure 4. Infrared spectra in the 950−740 cm^{-1} region from co-deposition of laser-evaporated scandium atoms with 0.025% $^{16}O_2$ + 0.05% $^{16}O^{18}O$ + 0.025% $^{18}O_2$ in argon: (a) 1.5 h of sample deposition at 6 K, (b) after 25 K annealing, (c) after 35 K annealing, and (d) after 15 min of 400 < λ < 580 nm irradiation.

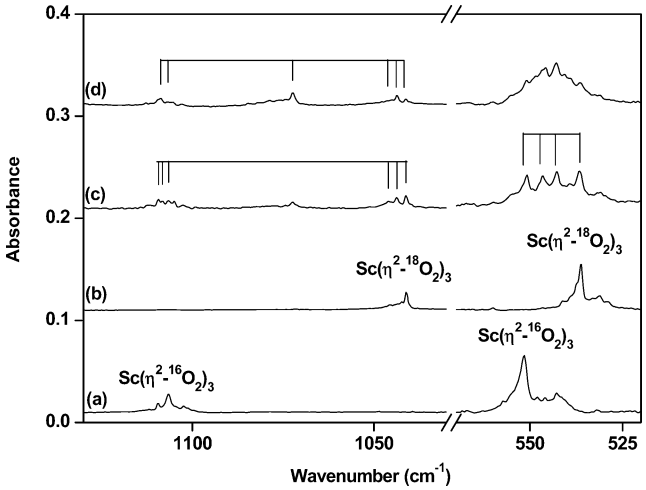

Figure 5. Infrared spectra in the 1130−1030 and 570−520 cm^{-1} regions from co-deposition of laser-evaporated scandium atoms with isotopic-labeled oxygen in excess argon. Spectra were taken after sample deposition followed by 35 K annealing and 15 min of 400 < λ < 580 nm irradiation: (a) 0.1% $^{16}O_2$, (b) 0.1% $^{18}O_2$, (c) 0.05% $^{16}O_2$ + 0.05% $^{18}O_2$, and (d) 0.025% $^{16}O_2$ + 0.05% $^{16}O^{18}O$ + 0.025% $^{18}O_2$.

the experiments, which suggests that these two absorptions are due to different vibrational modes of the same molecule. The 921.7 cm^{-1} absorption shifted to 883.0 cm^{-1} upon $^{16}O/^{18}O$ substitution, corresponding to an isotopic $^{16}O/^{18}O$ ratio of 1.0438. The band position and isotopic frequency ratio imply that the 921.7 cm^{-1} absorption is due to a terminal Sc═O stretching vibration. The spectra from the experiments with a 1:1 mixture of $^{16}O_2$ and $^{18}O_2$ (Figure 3) and a 1:2:1 mixture of $^{16}O_2$, $^{16}O^{18}O$, and $^{18}O_2$ (Figure 4) revealed that only one Sc═O fragment was involved in the 921.7 cm^{-1} mode. The 801.8 cm^{-1} absorption shifted to 758.1 cm^{-1} with $^{18}O_2$, exhibiting an isotopic $^{16}O/^{18}O$ ratio of 1.0576, which is characteristic of an O−O stretching vibration. As shown in Figures 3 and 4, four absorptions located at 801.8, 792.4, 767.0, and 758.1 cm^{-1} were observed in the experiment with a 1:1 mixture of $^{16}O_2$ and $^{18}O_2$, and six absorptions positioned at 801.8, 792.4, 782.6, 776.9, 767.0, and 758.1 cm^{-1} were resolved when the 1:2:1 mixture of $^{16}O_2$, $^{16}O^{18}O$, and $^{18}O_2$ was used. These spectral features are about the same as those of the antisymmetric stretching modes of the O_3^- anion and the recently reported OM(η^2-O_2)(η^2-O_3)

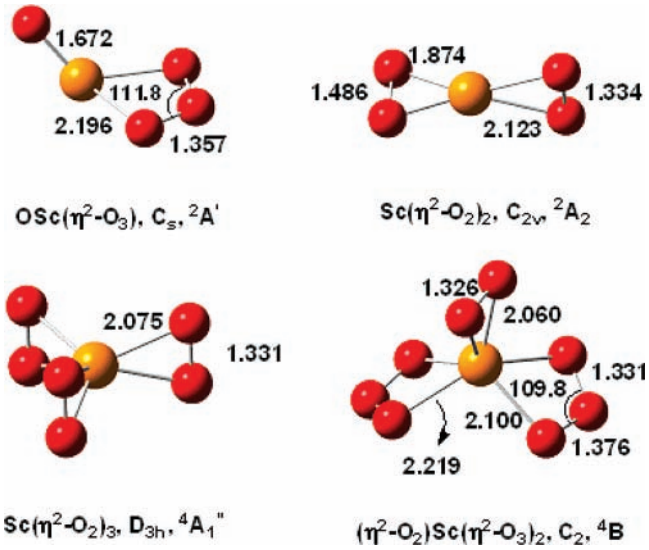

Figure 6. Optimized structures of the products (bond lengths in angstroms and bond angles in degrees).

(M = Ti, Zr, Hf) complexes in solid argon.[20,27] Accordingly, the 921.7 and 801.8 cm^{-1} absorptions are assigned to the Sc═O stretching and antisymmetric O_3 stretching modes of the OSc-(η^2-O_3) complex.

The assignment is supported by DFT calculations. As shown in Figure 6, the OSc(η^2-O_3) molecule was predicted to possess a nonplanar C_s symmetry with a doublet ground state. The O_3 subunit is side-on bonded to Sc in an η^2 fashion. The terminal Sc═O bond length was predicted to be 1.672 Å, very close to the values of the previously reported scandium monoxide complexes with dinitrogen and acetylene.[28] The Sc═O stretching and antisymmetric O_3 stretching vibrational frequencies were calculated at 975.9 and 842.8 cm^{-1}, respectively, with the isotopic frequency ratios in good agreement with the experimental values (Tables 2 and 3). The other modes such as the symmetric O_3 stretching and bending modes were predicted to have very low IR intensities (Table 2), and they were not able to be detected. The antisymmetric O_3 stretching vibrational mode observed at 801.8 cm^{-1} is very close to the O_3^- anion absorption at 804.3 cm^{-1} isolated in solid argon.[27] Hence, the OSc(η^2-O_3) complex can be regarded as [$(ScO)^+(O_3)^-$], a scandium monoxide cation coordinated by a side-on bonded O_3^- anion. Consistent with that notion, the calculated spin density is primarily localized on the O_3 fragment (0.99e). Bonding analysis indicates that the singly occupied molecular orbital is mainly the LUMO antibonding π orbital (b_1) of O_3 in character.

Additional calculations were performed on the Sc(η^2-O_3) complex, which was predicted to have a doublet ground state with a planar C_{2v} symmetry. The most intense IR absorption of Sc(η^2-O_3) was computed at 743.7 cm^{-1}, which is too low to fit the observed value of 801.8 cm^{-1}.

OSc(η^2-O_3)(O_2)$_x$. In the experiments employing relatively high O_2 concentrations, four absorptions in the low-frequency side of the 921.7 cm^{-1} absorption evolved on sample annealing at the expense of the 921.7 cm^{-1} absorption. These absorptions showed about the same isotopic frequency ratios as that of the 921.7 cm^{-1} absorption. In concert, the 801.8 cm^{-1} absorption is broadened and the band position shifted to 803.5 cm^{-1} upon sample annealing. The 919.0, 916.1, 913.8, and 911.9 cm^{-1} absorptions are assigned to the Sc═O stretching modes of the weakly bound OSc(η^2-O_3)(O_2)$_x$ complexes with x = 1−4. The antisymmetric O_3 stretching modes of these complexes were not able to be resolved.

TABLE 1: Infrared Absorptions (cm^{-1}) from the Reactions of Laser-Evaporated Scandium Atoms with Dioxygen in Solid Argon

$^{16}O_2$	$^{18}O_2$	$^{16}O_2 + {}^{18}O_2$	$^{16}O_2 + {}^{16}O^{18}O + {}^{18}O_2$	assignment
921.7	883.0	921.6, 883.5	921.4, 883.6	$OSc(\eta^2\text{-}O_3)$, Sc═O str.
801.8	758.1	801.8, 792.4, 767.0, 758.1	801.8, 792.4, 782.6 776.9, 767.0, 758.1	$OSc(\eta^2\text{-}O_3)$, O_3 asym str.
1102.4	1040.8			$Sc(\eta^2\text{-}O_2)_2$, superoxo O−O str.
836.0	797.0	836.0, 817.9, 815.4, 797.0	836.0, 818.0, 815.5, 797.0	$Sc(\eta^2\text{-}O_2)_2$, peroxo O−O str.
631.7	608.1			$Sc(\eta^2\text{-}O_2)_2$, sym. Sc−O_2 str.
612.7	584.2			$Sc(\eta^2\text{-}O_2)_2$, asym. Sc−O_2 str.
1106.7	1041.1	1109.4, 1108.3, 1106.7, 1043.8, 1046.0, 1041.1		$Sc(\eta^2\text{-}O_2)_3$, O−O str.
551.7	536.1	550.9, 546.6, 542.8, 536.7		$Sc(\eta^2\text{-}O_2)_3$, Sc−O_2 str.
818.7	774.2			$(\eta^2\text{-}O_2)Sc(\eta^2\text{-}O_3)_2$, asy. O_3 str.
681.2	645.4			$(\eta^2\text{-}O_2)Sc(\eta^2\text{-}O_3)_2$, sym. O_3 bend.
678.7	643.2			$(\eta^2\text{-}O_2)Sc(\eta^2\text{-}O_3)_2$, asym.$O_3$ bend.
544.6	528.5	543.6, 529.5	543.6, 537.6, 529.5	$(\eta^2\text{-}O_2)Sc(\eta^2\text{-}O_3)_2$, Sc−$O_2$ str.
919.0	880.6	919.1, 880.9	918.8, 881.0	$OSc(\eta^2\text{-}O_3)(O_2)_x$, Sc═O str.
916.1	877.9	916.2, 878.1	915.9, 878.2	$OSc(\eta^2\text{-}O_3)(O_2)_x$
913.8	875.5	913.6, 875.8	913.4, 875.8	$OSc(\eta^2\text{-}O_3)(O_2)_x$
911.9	873.6	911.7, 873.8	911.4, 874.0	$OSc(\eta^2\text{-}O_3)(O_2)_x$
803.5	759.3	803.7, 795.5, 769.4, 759.3	803.9, 795.5, 785.6, 779.3, 769.4, 759.3	$OSc(\eta^2\text{-}O_3)(O_2)_x$, asy. O_3 str.

TABLE 2: DFT/B3LYP Calculated Total Energies (in Hartree, after Zero-Point Energy Corrections), Frequencies (cm^{-1}), and Intensities (km/mol) of the Products and Transition State

molecule	energy	frequency (intensity)
$OSc(\eta^2\text{-}O_3)$ ($^2A'$, C_s)	−1061.594236	1064.2 (2), 975.9 (282), 842.8 (258), 670.6 (36), 343.0 (1), 327.5 (67), 209.2 (18), 124.9 (45), 102.6 (40)
$Sc(\eta^2\text{-}O_2)_2$ ($^2A_2$, C_{2v})	−1061.619355	1165.4 (41), 882.2 (184), 640.3 (65), 614.5 (31), 458.1 (8), 414.8 (27), 155.3 (0), 77.9 (54), 66.4 (72)
$Sc(\eta^2\text{-}O_2)_3$ ($^4A_1''$, D_{3h})	−1212.039861	1187.1 (0), 1167.3 (552), 528.6 (1262), 425.3 (4), 410.7 (02), 407.6 (0), 105.3 (62), 91.2 (0), 56.6 (02), 46.1 (39)
$(\eta^2\text{-}O_2)Sc(\eta^2\text{-}O_3)_2$ (^4B, C_2)	−1362.357780	1186.7 (29), 1097.5 (18), 1097.3 (4), 854.1 (332), 836.5 (3), 695.9 (32), 685.1 (94), 531.2 (125), 443.9 (65), 395.5 (75), 325.5 (4), 263.4 (6), 249.4 (5), 216.0 (3), 191.1 (1), 109.0 (5), 87.4 (9), 87.3 (0), 65.1 (2), 44.4 (0), 33.0 (0)
TS (^2A, C_1)	−1061.558488	1008.6 (133), 686.8 (214), 577.3 (52), 532.3 (16), 432.4 (15), 263.8 (11), 129.2 (39), 71.8 (63), 619.8i (90)

$Sc(\eta^2\text{-}O_2)_2$. The absorptions at 1102.4, 836.0, 631.7, and 612.7 cm^{-1} were produced under visible light ($400 < \lambda < 580$ nm) irradiation, during which the $OSc(\eta^2\text{-}O_3)$ absorptions were completely destroyed. This experimental observation suggests that the photolysis product belongs to a structural isomer of the $OSc(\eta^2\text{-}O_3)$ complex. These absorptions are assigned to different vibrational modes of the $Sc(\eta^2\text{-}O_2)_2$ complex. The 1102.4 cm^{-1} absorption is weak; it shifted to 1040.8 cm^{-1} when the isotopic $^{18}O_2$ sample was used. The band position and isotopic ratio of 1.0592 indicate that it is an O−O stretching mode of a superoxo ligand.[29] The 836.0 cm^{-1} absorption is due to an O−O stretching mode of a peroxo ligand.[29] The isotopic $^{16}O/^{18}O$ ratio of 1.0489 is lower than that of pure O−O stretching mode, which suggests mode mixing with the low-energy Sc−O_2 stretching mode. The 631.7 and 612.7 cm^{-1} absorptions are mainly due to the Sc−O_2 stretching modes of the peroxo ligand.

As shown in Figure 6, the $Sc(\eta^2\text{-}O_2)_2$ complex has a doublet ground state ($^2A_2$) with a C_{2v} symmetry, in which the superoxo ScO_2 plane is perpendicular to the peroxo ScO_2 plane. The two O−O bond distances were predicted to be 1.334 and 1.486 Å, which fall into the superoxide and peroxide categories, respectively.[29] Therefore, $Sc(\eta^2\text{-}O_2)_2$ is a superoxo scandium peroxide complex, which can be regarded as $[Sc^{3+}(O_2^-)(O_2^{2-})]$, that is, a scandium trication coordinated by an O_2^- anion and an O_2^{2-} anion. Population analysis showed that the unpaired electron is located on the superoxo ligand (1.03e). In the previous matrix isolation experiments, a 552.6 cm^{-1} absorption was assigned to the $Sc(\eta^2\text{-}O_2)_2$ complex with a D_{2d} symmetry[13] analogous to the $Ca(\eta^2\text{-}O_2)_2$ molecule.[30] As will be discussed below, the 551.7 cm^{-1} absorption observed in present experiments corresponds to the previously reported 552.6 cm^{-1} absorption, and it is reassigned to the $Sc(\eta^2\text{-}O_2)_3$ complex. Calcium has two valent electrons with the highest oxidation state of +2, and it is able to form bis-superoxide complex with two equivalent superoxo ligands, which satisfies its +2 oxidation state.[30] In contrast, scandium has three valence electrons with an oxidation state of +3, and it prefers to form trivalent species. The $Sc(\eta^2\text{-}O_2)_2$ complex with a side-on bonded superoxo O_2^- ligand and a side-on bonded peroxo O_2^{2-} ligand is the most stable structure when scandium is coordinated by two O_2 molecules. We also performed theoretical calculations on the other $Sc(\eta^2\text{-}O_2)_2$ isomers with D_{2h} and D_{2d} symmetry. Both structures were predicted to be transition states with quite large imaginary frequencies corresponding to reduce the symmetry to two inequivalent O_2 subunits. As listed in Table 3, the calculated vibrational frequecnies and isotopic frequency ratios of the C_{2v} $Sc(\eta^2\text{-}O_2)_2$ complex fit the experimental values quite well, which support the experimental assignment.

$Sc(\eta^2\text{-}O_2)_3$. The 1106.7 and 551.7 cm^{-1} absorptions appeared together on annealing. The 551.7 cm^{-1} absorption shifted to 536.1 cm^{-1} with $^{18}O_2$. The band position and isotopic frequency ratio of 1.0291 imply that this absorption is due to a Sc−O_2 stretching mode. In the experiment with a 1:1 mixture of $^{16}O_2$ and $^{18}O_2$, a quartet located at 550.9, 546.6, 542.8, and 536.7 cm^{-1} was produced (Figure 5). This spectral feature indicates that it is a doubly degenerate vibrational mode with three equivalent O_2 subunits. The 1106.7 cm^{-1} absorption exhibited an isotopic frequency ratio of 1.0630. The band position and isotopic frequency ratio indicate that this absorption is due to

TABLE 3: Comparison between the Observed and Calculated Vibrational Frequencies (cm^{-1}) and Isotopic Frequency Ratios of the Product Molecules

		freq		$^{16}O/^{18}O$	
molecule	mode	calcd	obsd	calcd	obsd
$OSc(\eta^2\text{-}O_3)$ ($^2A'$)	Sc═O stretch (a′)	975.9	921.7	1.0442	1.0438
	O_3 asym. stretch (a″)	842.8	801.8	1.0605	1.0576
$Sc(\eta^2\text{-}O_2)_2$ ($^2A_2$)	superoxo O_2 stretch (a_1)	1165.4	1102.4	1.0608	1.0592
	peroxo O_2 stretch (a_1)	882.2	836.0	1.0519	1.0489
	Sc−O_2 sym. stretch (a_1)	640.3	631.7	1.0383	1.0388
	Sc−O_2 asym. stretch (b_2)	614.5	612.7	1.0519	1.0488
$Sc(\eta^2\text{-}O_2)_3$ ($^4A_1''$)	O−O stretch (e′)	1167.3	1106.7	1.0608	1.0630
	Sc−O_2 stretch (e′)	528.6	551.7	1.0262	1.0291
$(\eta^2\text{-}O_2)Sc(\eta^2\text{-}O_3)_2$ (^4B)	O_3 asym. stretch (b)	854.1	818.7	1.0599	1.0575
	sym. O_3 bending (a)	695.9	681.2	1.0600	1.0555
	asym.O_3 bending (b)	685.1	678.7	1.0586	1.0552
	Sc−O_2 stretch (a)	531.2	544.6	1.0291	1.0305

the O−O stretching mode of a superoxo ligand.[29] In the experiment with an equal molar mixture of $^{16}O_2$ and $^{18}O_2$, two weak intermediate absorptions between the pure isotopic counterparts (1046.0 and 1043.8 cm^{-1}) together with two additional weak absorptions above the 1106.7 cm^{-1} (1109.4 and 1108.3 cm^{-1}) were observed, which also suggests the involvement of three equivalent O_2 subunits. Accordingly, we assign the 1106.7 and 551.7 cm^{-1} absorptions to the $Sc(\eta^2\text{-}O_2)_3$ complex. The observation of only one O−O stretching mode implies that the complex is centrosymmetric.

To validate the assignment, DFT calculations were performed. The $Sc(\eta^2\text{-}O_2)_3$ complex was predicted to have a $^4A_1''$ ground state with a D_{3h} symmetry with three side-on bonded O_2 ligands around the scandium atom, which thus presents a 6-fold coordination. (Figure 6). The O−O bond length was predicted to be 1.331 Å. This oxygen-rich complex can be viewed as $[Sc^{3+}(O_2^-)_3]$, that is, a side-on bonded homoleptic trisuperoxo scandium complex. Population analysis indicates that the three unpaired electrons are distributed on the three equivalent O_2^- fragments (1.06e each). The two experimentally observed vibrational modes were computed at 1167.3 and 528.6 cm^{-1} (Table 2) with isotopic shifts and splitting in good agreement with the experimental observations. According to calculation, the antisymmetric O−O stretching mode should split into a quartet at 1167.3, 1111.6, 1105.6, and 1100.6 cm^{-1} with approximately 275:72:117:250 km/mol relative intensities in the experiment with an equal molar mixture of $^{16}O_2$ and $^{18}O_2$. The symmetric O−O stretching mode was predicted at 1187.1 cm^{-1} with zero IR intensity. However, this mode becomes IR active in partially isotopic substituted isotopomers. The 1109.4 and 1108.3 cm^{-1} absorptions observed in the $^{16}O_2 + {}^{18}O_2$ experiment are due to the symmetric O−O stretching modes of the $Sc(\eta^2\text{-}{}^{18}O_2)_2(\eta^2\text{-}{}^{16}O_2)$ and $Sc(\eta^2\text{-}{}^{18}O_2)(\eta^2\text{-}{}^{16}O_2)_2$ isotopomers, which were predicted at 1181.6 and 1175.2 cm^{-1} with 39 and 87 km/mol IR intensities.

Recent matrix isolation investigation of thermally evaporated aluminum atoms with O_2 gave the $Al(\eta^2\text{-}O_2)_3$ complex, which was characterized to be a 6-fold coordinated trisuperoxo complex. The O−O and Al−O_2 stretching vibrational modes were observed at 1065 and 686 cm^{-1}, respectively.[31] Scandium is isovalent with aluminum and, hence, is able to form the $Sc(\eta^2\text{-}O_2)_3$ complex. More recent investigation in this laboratory on the reaction of hafnium with dioxygen has characterized an 8-fold coordinated tetrasuperoxo hafnium complex, $Hf(\eta^2\text{-}O_2)_4$, as hafnium has four valence electrons with the highest oxidation state of +4.[20]

$(\eta^2\text{-}O_2)Sc(\eta^2\text{-}O_3)_2$. The 818.7 and 544.6 cm^{-1} absorptions appeared together on annealing in the experiments using high O_2 concentrations. These two absorptions dominate the spectrum after high-temperature annealing. The band position and isotopic frequency ratio (1.0575) imply that the 818.7 cm^{-1} absorption is due to an O−O stretching mode of O_3 ligands. The spectral features in the experiments with the $^{16}O_2 + {}^{18}O_2$ and $^{16}O_2 + {}^{16}O^{18}O + {}^{18}O_2$ mixtures were not able to be resolved due to isotopic dilution, which suggests the involvement of more than one O_3 subunit. The 544.6 cm^{-1} absorption shifted to 528.5 cm^{-1} with an isotopic ratio of 1.0305. In the mixed $^{16}O_2 + {}^{18}O_2$ experiment, only two absorptions were observed with the band positions slightly shifted from the positions observed in the experiments using $^{16}O_2$ and $^{18}O_2$ separately. When the mixed $^{16}O_2 + {}^{16}O^{18}O + {}^{18}O_2$ sample was used, an intermediate absorption at 537.6 cm^{-1} was observed. The band position and isotopic spectral features indicate this band is due to a Sc−O_2 stretching mode with only one O_2 fragment involvement. Accordingly, the 818.7 and 544.6 cm^{-1} absorptions are assigned to the $(\eta^2\text{-}O_2)Sc(\eta^2\text{-}O_3)_2$ complex. Two weak absorptions at 681.2 and 678.7 cm^{-1} are due to the Sc−O_3 bending vibrations of the complex.

DFT calculations on $(\eta^2\text{-}O_2)Sc(\eta^2\text{-}O_3)_2$ gave a ^4B ground state with a C_2 symmetry (Figure 6). At the optimized structure, the O_2 fragment is side-on bonded with an O−O bond length of 1.326 Å, which is due to a superoxo ligand.[29] The two O_3 subunits are equivalent and are also side-on bonded with the O−O bond lengths of 1.376 and 1.331 Å, respectively. The $(\eta^2\text{-}O_2)Sc(\eta^2\text{-}O_3)_2$ complex can be considered as $[Sc^{3+}(O_2^-)(O_3^-)_2]$, a 6-fold coordinated superoxo scandium bisozonide complex. The antisymmetric O_3 stretching and the Sc−O_2 bending modes were calculated at 854.1 and 531.2 cm^{-1}. These two modes were predicted to have the highest IR intensities. The O−O stretching mode of the superoxo ligand was computed at 1186.7 cm^{-1} with quite low IR intensity (Table 2) and was not observed.

It should be pointed out that the above-characterized scandium oxide/dioxygen complexes may be coordinated by argon atom(s) in solid argon matrix. Recent studies indicated that some transition metal as well as f element metal compounds trapped in solid matrixes are not "isolated" but are coordinated by multiple noble gas atoms.[26,32−36] It is difficult to determine whether the above-characterized species are coordinated by argon atoms or not experimentally, but some information can be drawn from theoretical calculations. We will take the $Sc(\eta^2\text{-}O_2)_2$ as an example to discuss argon coordination. As shown in Figure 4, the peroxo ligand O−O stretching mode of $Sc(\eta^2\text{-}$

$O_2)_2$ splits into a quartet with two closely located intermediates in the experiment with a 1:2:1 $^{16}O_2 + {}^{16}O^{18}O + {}^{18}O_2$ sample, which suggests that the two O atoms are slightly inequivalent. This suggests that the Sc(η^2-$O_2)_2$ complex may coordinated by argon atom(s) in a solid argon matrix. DFT calculations show that the $^2A_2$ state of Sc(η^2-$O_2)_2$ can at least coordinate two Ar atoms in forming an ^2A state Ar_2-Sc(η^2-$O_2)_2$ complex. The predicted O−O stretching modes are only slightly shifted upon Ar coordination (883.3 and 1168.1 cm^{-1} versus 882.2 and 1165.4 cm^{-1}). However, the two O atoms of the peroxo ligand become inequivalent upon Ar coordination, which results in two intermediates (1.0 cm^{-1} separation) in the calculated spectra with mixed $^{16}O_2 + {}^{16}O^{18}O + {}^{18}O_2$ sample.

Reaction Mechanism. It has been shown in the previous experiments that early transition metal atoms (Ti−Cr) reacted spontaneously with dioxygen to form the OMO molecules in solid matrixes.[37−39] In agreement with previous studies,[13,14] no neutral OScO was observed in the present experiments. The behavior of the product absorptions suggests that the ground state scandium atoms are able to react with $(O_2)_2$ van der Waals dimer complex or two O_2 molecules in solid argon to form the OSc(η^2-O_3) complex, reaction 1, which requires no activation energy. The calculations indicate the OSc(η^2-O_3) complex is about 150.8 kcal/mol more stable than the separated reactants: Sc + $2O_2$. At high O_2 concentration experiments, the OSc(η^2-O_3) complex can further react with dioxygen to form the OSc-(η^2-O_3)$(O_2)_x$ ($x = 1-4$) complexes.

$$\mathrm{Sc}\ (^2\mathrm{D}) + 2\mathrm{O}_2\ (^3\Sigma_g^-) \rightarrow \mathrm{OSc}(\eta^2\text{-}\mathrm{O}_3)\ (^2\mathrm{A}') \qquad \Delta E = -150.8\ \mathrm{kcal/mol} \quad (1)$$

The OSc(η^2-O_3) absorptions disappeared under visible light irradiation, during which the Sc(η^2-$O_2)_2$ complex absorptions were produced. This observation suggests that the OSc(η^2-O_3) complex underwent photochemical isomerization to form the Sc(η^2-$O_2)_2$ isomer. The Sc(η^2-$O_2)_2$ complex was predicted to be 15.8 kcal/mol more stable than the OSc(η^2-O_3) complex. The OSc(η^2-O_3) → Sc(η^2-$O_2)_2$ isomerization reaction was predicted to proceed via a transition state lying about 22.4 kcal/mol higher in energy than the OSc(η^2-O_3) complex (reaction 2). Therefore, this isomerization reaction proceeded only under visible light irradiation, during which some exited states are involved. Our DFT calculations predicted a $^4B_1$ state lies 69.8 kcal/mol (around 410 nm) above the doublet ground state of OSc(η^2-O_3).

$$\mathrm{OSc}(\eta^2\text{-}\mathrm{O}_3)\ (^2\mathrm{A}') \rightarrow \mathrm{Sc}(\eta^2\text{-}\mathrm{O}_2)_2\ (^2\mathrm{A}_2) \qquad \Delta E = -15.8\ \mathrm{kcal/mol} \quad (2)$$

The absorptions due to the Sc(η^2-$O_2)_3$ and (η^2-O_2)Sc(η^2-$O_3)_2$ complexes were also produced upon sample annealing with high O_2 concentrations. These oxygen-rich species were formed by the reactions of OSc(η^2-O_3) and O_2 via the OSc(η^2-O_3)$(O_2)_x$ intermediates, reactions 3 and 4, which were predicted to be exothermic by 49.6 and 19.0 kcal/mol, respectively. The Sc-(η^2-$O_2)_3$ and (η^2-O_2)Sc(η^2-$O_3)_2$ absorptions increased upon sample annealing, which suggests that reactions 3 and 4 require very low activation energies.

$$\mathrm{OSc}(\eta^2\text{-}\mathrm{O}_3)\ (^2\mathrm{A}') + \mathrm{O}_2\ (^3\Sigma_g^-) \rightarrow \mathrm{OSc}(\eta^2\text{-}\mathrm{O}_3)(\mathrm{O}_2) \rightarrow \mathrm{Sc}(\eta^2\text{-}\mathrm{O}_2)_3\ (^4\mathrm{A}_1'') \quad (3)$$

$$\mathrm{OSc}(\eta^2\text{-}\mathrm{O}_3)\ (^2\mathrm{A}') + 2\mathrm{O}_2\ (^3\Sigma_g^-) \rightarrow \mathrm{OSc}(\eta^2\text{-}\mathrm{O}_3)(\mathrm{O}_2)_2 \rightarrow (\eta^2\text{-}\mathrm{O}_2)\mathrm{Sc}(\eta^2\text{-}\mathrm{O}_3)_2\ (^4\mathrm{B}) \quad (4)$$

Conclusions

The reactions of scandium atoms with dioxygen have been reinvestigated using matrix isolation infrared spectroscopy and density functional theory calculations. Laser-evaporated scandium atoms were co-deposited with dioxygen in excess argon at 6 K. Sample annealing allows the O_2 molecules in solid argon to diffuse and react with the ground state scandium atoms to form the OSc(η^2-O_3) complex, a side-on bonded scandium monoxide ozonide complex. The OSc(η^2-O_3) complex can further react with dioxygen to form the weakly bound OSc(η^2-O_3)$(O_2)_x$ ($x = 1-4$) complexes. The OSc(η^2-O_3) complex rearranges to a more stable Sc(η^2-$O_2)_2$ isomer under visible light irradiation, which is characterized to be a side-on bonded superoxo scandium peroxide complex, $[Sc^{3+}(O_2^-)(O_2^{2-})]$. On sample annealing, OSc(η^2-O_3)$(O_2)_x$ complexes rearrange to the homoleptic trisuperoxo scandium complex, Sc(η^2-$O_2)_3$, and the superoxo scandium bisozonide complex, (η^2-O_2)Sc(η^2-$O_3)_2$. The Sc(η^2-$O_2)_3$ complex is determined to have a D_{3h} symmetry with three equivalent side-on bonded superoxo ligands around the scandium atom, which thus presents a 6-fold coordination. The (η^2-O_2)Sc(η^2-$O_3)_2$ complex has a C_2 symmetry with two equivalent side-on bonded O_3 ligands and one side-on bonded superoxo ligand. These oxygen-rich complexes are potential important intermediates in transition metal oxidations under high O_2 concentrations.

Acknowledgment. This work is supported by the National Basic Research Program of China (2004CB719501 and 2007CB815203) and the Committee of Science and Technology of Shanghai (04JC14016).

References and Notes

(1) See, for examples: (a) Bortolini, O.; Conte, V. *J. Inorg. Biochem.* **2005**, *99*, 1549. (b) Bakac, A. *Adv. Inorg. Chem.* **2004**, *55*, 1. (c) Costas, M.; Mehn, M. P.; Jensen, M. P.; Que, L., Jr. *Chem. Rev.* **2004**, *104*, 939. (d) Mukhopadhyay, S.; Mandal, S. K.; Bhaduri, S.; Armstrong, W. H. *Chem. Rev.* **2004**, *104*, 3981. (e) Que, L., Jr.; Tolman, W. B. *Angew. Chem., Int. Ed.* **2002**, *41*, 1114.

(2) Dai, B.; Deng, K. M.; Yang, J. L.; Zhu, Q. S. *J. Chem. Phys.* **2003**, *118*, 9608.

(3) (a) Bauschlicher, C. W., Jr.; Langhoff, S. R. *J. Chem. Phys.* **1986**, *85*, 5936. (b) Bauschlicher, C. W., Jr.; Maitre, P. *Theor. Chim. Acta* **1995**, *90*, 189.

(4) Bakalbassis, E. G.; Stiakaki, M. A. D.; Tsipis, A. C.; Tsipis, C. A. *Chem. Phys.* **1996**, *205*, 389.

(5) Mattar, S. M. *J. Phys. Chem.* **1993**, *97*, 3171.

(6) Jeung, G. H.; Koutecký, J. *J. Chem. Phys.* **1988**, *88*, 3747.

(7) Dolg, M.; Wedig, U.; Stoll, H.; Preuss, H. *J. Chem. Phys.* **1987**, *86*, 2123.

(8) Andzelm, J.; Radzio, E.; Barandiarán, Z.; Seijo, L. *J. Chem. Phys.* **1985**, *83*, 4565.

(9) (a) Shirley, J.; Scurlock, C.; Steimle, T. *J. Chem. Phys.* **1990**, *93*, 1568. (b) Rice, S. F.; Childs, W. J.; Field, R. W. *J. Mol. Spectrosc.* **1989**, *133*, 22. (c) Childs, W. J.; Steimle, T. *J. Chem. Phys.* **1988**, *88*, 6168. (d) Rice, S. F.; Field, R. W. *J. Mol. Spectrosc.* **1986**, *119*, 331.

(10) Merer, A. J. *Annu. Rev. Phys. Chem.* **1989**, *40*, 407.

(11) Weltner, W., Jr.; McLeod, D., Jr.; Kasai, P. H. *J. Chem. Phys.* **1967**, *46*, 3172.

(12) (a) Gutsev, G. L.; Andrews, L.; Bauschlicher, C. W., Jr. *Theor. Chem. Acc.* **2003**, *109*, 298. (b) Knight, L. B.; Kaup, J. G.; Petzoldt, B.; Ayyad, R.; Ghanty, T. K.; Davidson, E. R. *J. Chem. Phys.* **1999**, *110*, 5658.

(13) Chertihin, G. V.; Andrews, L.; Rosi, M.; Bauschlicher, C. W., Jr. *J. Phys. Chem. A* **1997**, *101*, 9085.

(14) Bauschlicher, C. W., Jr.; Zhou, M. F.; Andrews, L.; Johnson, J. R. T.; Panas, I.; Snis, A.; Roos, B. O. *J. Phys. Chem. A* **1999**, *103*, 5463.

(15) Gutsev, G. L.; Rao, B. K.; Jena, P. *J. Phys. Chem. A* **2000**, *104*, 11961.

(16) Gonzales, J. M.; King, R. A.; Schaefer, H. F., III. *J. Chem. Phys.* **2000**, *113*, 567.

(17) Kim, S. J.; Crawford, T. D. *J. Phys. Chem. A* **2004**, *108*, 3097.

(18) Rosi, M.; Bauschlicher, C. W.; Chertihin, G. V.; Andrews, L. *Theor. Chem. Acc.* **1998**, *99*, 106.

(19) Wu, H. B.; Wang, L. S. *J. Phys. Chem. A* **1998**, *102*, 9129.

(20) (a) Gong, Y.; Zhou, M. F.; Tian, S. X.; Yang, J. L. *J. Phys. Chem. A* **2007**, *111*, 6127. (b) Gong, Y.; Zhou, M. F. *J. Phys. Chem. A* **2007**, *111*, 8973.

(21) (a) Wang, G. J.; Gong, Y.; Chen, M. H.; Zhou, M. F. *J. Am. Chem. Soc.* **2006**, *128*, 5974. (b) Zhou, M. F.; Tsumori, N.; Xu, Q.; Kushto, G. P.; Andrews, L. *J. Am. Chem. Soc.* **2003**, *125*, 11371. (c) Zhou, M. F.; Andrews, L.; Bauschlicher, C. W., Jr. *Chem. Rev.* **2001**, *101*, 1931.

(22) *Gaussian 03, Revision B.05*; Frisch, M. J.; Trucks, G. W.; Schlegel, H. B.; Scuseria, G. E.; Robb, M. A.; Cheeseman, J. R.; Montgomery, J. A., .; Vreven, T.; Kudin, K. N.; Burant, J. C.; Millam, J. M.; Iyengar, S. S.; Tomasi, J.; Barone, V.; Mennucci, B.; Cossi, M.; Scalmani, G.; Rega, N.; Petersson, G. A.; Nakatsuji, H.; Hada, M.; Ehara, M.; Toyota, K.; Fukuda, R.; Hasegawa, J.; Ishida, M.; Nakajima, T.; Honda, Y.; Kitao, O.; Nakai, H.; Klene, M.; Li, X.; Knox, J. E.; Hratchian, H. P.; Cross, J. B.; Adamo, C.; Jaramillo, J.; Gomperts, R.; Stratmann, R. E.; Yazyev, O.; Austin, A. J.; Cammi, R.; Pomelli, C.; Ochterski, J. W.; Ayala, P. Y.; Morokuma, K.; Voth, G. A.; Salvador, P.; Dannenberg, J. J.; Zakrzewski, V. G.; Dapprich, S.; Daniels, A. D.; Strain, M. C.; Farkas, O.; Malick, D. K.; Rabuck, A. D.; Raghavachari, K.; Foresman, J. B.; Ortiz, J. V.; Cui, Q.; Baboul, A. G.; Clifford, S.; Cioslowski, J.; Stefanov, B. B.; Liu, G.; Liashenko, A.; Piskorz, P.; Komaromi, I.; Martin, R. L.; Fox, D. J.; Keith, T.; Al-Laham, M. A.; Peng, C. Y.; Nanayakkara, A.; Challacombe, M.; Gill, P. M. W.; Johnson, B.; Chen, W.; Wong, M. W.; Gonzalez, C.; Pople, J. A. Gaussian, Inc.: Pittsburgh, PA, 2003.

(23) Becke, A. D. *J. Chem. Phys.* **1993**, *98*, 5648.

(24) Lee, C.; Yang, W.; Parr, R. G. *Phys. Rev. B* **1988**, *37*, 785.

(25) (a) McLean, A. D.; Chandler, G. S. *J. Chem. Phys.* **1980**, *72*, 5639. (b) Krishnan, R.; Binkley, J. S.; Seeger, R.; Pople, J. A. *J. Chem. Phys.* **1980**, *72*, 650.

(26) (a) Zhao, Y. Y.; Wang, G. J.; Chen, M. H.; Zhou, M. F. *J. Phys. Chem. A* **2005**, *109*, 6621. (b) Zhao, Y. Y.; Gong, Y.; Chen, M. H.; Ding, C. F.; Zhou, M. F. *J. Phys. Chem. A* **2005**, *109*, 11765.

(27) (a) Wight, C. A.; Ault, B., S.; Andrews, L. *J. Chem. Phys.* **1976**, *65*, 1244. (b) Andrews, L.; Ault, B. S.; Grzybowski, J. M.; Allen, R. O. *J. Chem. Phys.* **1975**, *62*, 2461.

(28) (a) Zhou, M. F.; Wang, G. J.; Zhao, Y. Y.; Chen, M. H.; Ding, C. F. *J. Phys. Chem. A* **2005**, *109*, 5079. (b) Wang, G. J.; Chen, M. H.; Zhao, Y. Y.; Zhou, M. F. *Chem. Phys.* **2006**, *322*, 354.

(29) (a) Cramer, C. J.; Tolman, W. B.; Theopold, K. H.; Rheingold, A. L. *Proc. Natl. Acad. Sci. U.S.A.* **2003**, *100*, 3635. (b) Hill, H. A. O.; Tew, D. G. *Comprehensive Coordination Chemistry*; Wilkinson, G., Gillard, R. D., McCleverty, J. A., Eds.; Pergamon, Oxford, **1987**; Vol. 2, p 315. (c) Vaska, L. *Acc. Chem. Res.* **1976**, *9*, 175. (d) Valentine, J. S. *Chem. Rev.* **1973**, *73*, 235.

(30) Andrews, L.; Chertihin, G. V.; Thompson, C. A.; Dillon, J.; Byrne, S.; Bauschlicher, C. W., Jr. *J. Phys. Chem.* **1996**, *100*, 10088.

(31) Stösser, G.; Schnöckel, H. *Angew. Chem., Int. Ed.* **2005**, *44*, 4261.

(32) Li, J.; Bursten, B. E.; Liang, B.; Andrews, L. *Science* **2002**, *295*, 2242.

(33) (a) Andrews, L.; Liang, B. Y.; Li, J.; Bursten, B. E. *J. Am. Chem. Soc.* **2003**, *125*, 3126. (b) Andrews, L.; Liang, B. Y.; Li, J.; Bursten, B. E. *Angew. Chem., Int. Ed.* **2000**, *39*, 4565.

(34) (a) Li, J.; Bursten, B. E.; Andrews, L.; Marsden, C. J. *J. Am. Chem. Soc.* **2004**, *126*, 3424. (b) Wang, X. F.; Andrews, L.; Li, J.; Bursten, B. E. *Angew. Chem., Int. Ed.* **2004**, *43*, 2554.

(35) (a) Zhao, Y. Y.; Gong, Y.; Chen, M. H.; Zhou, M. F. *J. Phys. Chem. A* **2006**, *110*, 1845. (b) Zhao, Y. Y.; Gong, Y.; Zhou, M. F. *J. Phys. Chem. A* **2006**, *110*, 10777. (c) Yang, R.; Gong, Y.; Zhou, H.; Zhou, M. F. *J. Phys. Chem. A* **2007**, *111*, 64.

(36) Jin, X.; Jiang, L.; Xu, Q.; Zhou, M. F. *J. Phys. Chem. A* **2006**, *110*, 12585.

(37) Chertihin, G. V.; Andrews, L. *J. Phys. Chem.* **1995**, *99*, 6356.

(38) Chertihin, G. V.; Bare, W. D.; Andrews, L. *J. Phys. Chem. A* **1997**, *101*, 5090.

(39) (a) Chertihin, G. V.; Bare, W. D.; Andrews, L. *J. Chem. Phys.* **1997**, *107*, 2798. (b) Zhou, M. F.; Andrews, L. *J. Chem. Phys.* **1999**, *111*, 4230.